

Title	System identification of propagating wave segments in excitable media and its application to advanced control
Author(s)	Katsumata, Hisatoshi; Konishi, Keiji; Hara, Naoyuki
Editor(s)	
Citation	Physical Review E. 2018, 97 (4), p.042210-1-042210-6
Issue Date	2018-04-17
URL	http://hdl.handle.net/10466/16069
Rights	©2018 American Physical Society

System identification of propagating wave segments in excitable media and its application to advanced control

Hisatoshi Katsumata, Keiji Konishi,* and Naoyuki Hara

Department of Electrical and Information Systems, Osaka Prefecture University, 1-1 Gakuen-cho, Naka-ku, Sakai, Osaka 599-8531 Japan

(Received 25 August 2017; revised manuscript received 8 January 2018; published 17 April 2018)

The present paper proposes a scheme for controlling wave segments in excitable media. This scheme consists of two phases: in the first phase, a simple mathematical model for wave segments is derived using only the time series data of input and output signals for the media; in the second phase, the model derived in the first phase is used in an advanced control technique. We demonstrate with numerical simulations of the Oregonator model that this scheme performs better than a conventional control scheme.

DOI: [10.1103/PhysRevE.97.042210](https://doi.org/10.1103/PhysRevE.97.042210)

I. INTRODUCTION

Excitable media have received considerable attention due to their wide range of applications. For example, cardiac arrhythmias can be modeled as spirals and turbulence occurring in excitable media [1,2], and the propagating waves in excitable media have the potential to be used for the realization of chemical information processing [3–5] and for finding optimal paths [6].

The elimination and control of turbulence, spirals, and propagating waves in excitable media have been widely studied. Recent studies have shown that these phenomena can be eliminated by external forces without feedback [7–11] or with feedback [12–14]. In addition to elimination, the control of waves and patterns in excitable media has also been actively investigated [15,16]. It was demonstrated experimentally that proportional (P) feedback control can stabilize a propagating wave segment in a photosensitive Belousov-Zhabotinsky chemical reaction system [17], and wave segment stabilization with P control has been analyzed in detail [18,19]. It was shown that a wave segment stabilized with P control can propagate along a desired path [20], and that multiple wave segments stabilized with proportional-integral-derivative (PID) control can be manipulated [21,22].

It has been analytically shown that it is difficult to specify the size of the wave segment that is stabilized with P control [23]. Our previous study demonstrated in numerical simulations that proportional-integral (PI) control, a common scheme in control engineering [24], can overcome this drawback [23]. Although PI control does not require a mathematical model of the controlled object, this control scheme will not perform well. This is a significant obstacle to the use of the control scheme. It is generally known in the field of control engineering that good performances can be obtained by controllers which are preliminarily designed based on a simple mathematical model described by the transfer function or the state-space representation. Unfortunately, it is difficult to analytically derive the simple mathematical model for wave segments in

excitable media. As a result, at the present stage, we are not able to control the wave segments with good performance. This difficulty is a bottleneck in the development of controlling excitable media.

The present paper tackles the above problem in two phases: in the first phase, to remove the bottleneck, the simple mathematical model (i.e., the transfer function) for wave segments is numerically derived using the prediction-error identification method [25,26], a popular numerical approach in control engineering. This method uses only the time series of input and output data of excitable media but does not use any other information about the media models, such as the dimension, nonlinearity, parameters, and so on. In the second phase, the controllers are preliminarily designed based on the model by the two-degrees-of-freedom compensation scheme [27], which is an advanced control technique. The designed controllers are applied to the wave segments in excitable media. These two phases are illustrated with numerical simulations of the Oregonator model [17,28].

II. EXCITABLE MEDIA WITH PI CONTROL

This section reviews our previous study [23] on PI control of propagating wave segments in excitable media. We consider an excitable medium,

$$\Sigma : \begin{cases} \frac{\partial u}{\partial t} = F(u, v, U) + D\nabla^2 u \\ \frac{\partial v}{\partial t} = G(u, v, U) \end{cases}, \quad (1)$$

where $u := u(t, \mathbf{x})$ and $v := v(t, \mathbf{x})$ are the activator and the inhibitor variables, respectively, at position $\mathbf{x} := (x_1, x_2) \in [0, L_1] \times [0, L_2]$ at time $t \in \mathbb{R}$. The size of the medium is defined by $L_{1,2} > 0$. The medium Σ has a spatially uniform input signal $U := U(t)$. The dynamics of the reactors are governed by $F, G : \mathbb{R} \times \mathbb{R} \times \mathbb{R} \rightarrow \mathbb{R}$. This paper employs the Oregonator model [17,28] for these functions (see Appendix). The medium Σ has diffusion coefficient $D \geq 0$ and Laplacian operator $\nabla^2 := \partial^2/\partial x_1^2 + \partial^2/\partial x_2^2$.

*<http://www.eis.osakafu-u.ac.jp/~ecs>

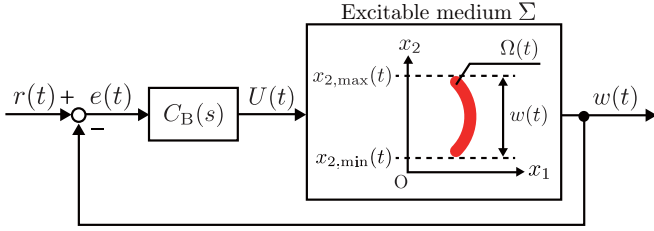


FIG. 1. Feedback system with PI control [23].

The present paper considers the excited area with the threshold $\bar{u} \in \mathbb{R}$,

$$\Omega(t) := \{\mathbf{x} \in [0, L_1] \times [0, L_2] : u(t, \mathbf{x}) \geq \bar{u}\}, t > 0, \quad (2)$$

as sketched in Fig. 1. The width of the propagating wave segment, $w(t) \in \mathbb{R}$, in the excitable medium Σ is used as the output signal [23]:

$$\begin{aligned} w(t) &:= x_{2,\max}(t) - x_{2,\min}(t), \\ x_{2,\max}(t) &:= \max_{\mathbf{x} \in \Omega(t)} x_2, \quad x_{2,\min}(t) := \min_{\mathbf{x} \in \Omega(t)} x_2. \end{aligned}$$

The spatially uniform input signal $U(t)$ is provided by the PI controller,

$$\begin{cases} U(t) &= K_P e(t) + z(t) \\ \frac{dz(t)}{dt} &= K_I e(t) \end{cases}, \quad (3)$$

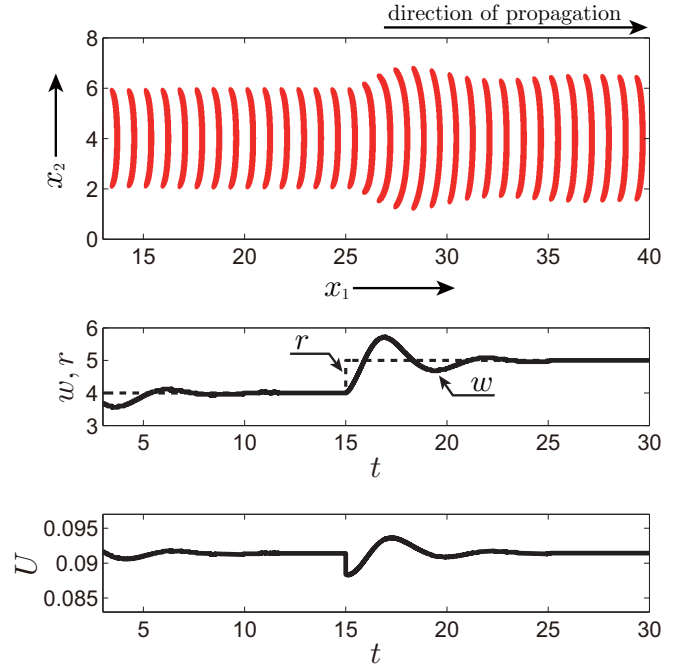
which has the additional state variable $z(t) \in \mathbb{R}$ and feedback gains $K_{P, I} \in \mathbb{R}$. The error is defined by $e(t) := r(t) - w(t)$, where $r(t) \in \mathbb{R}$ is the reference signal. The frequency domain description of this controller is given by

$$C_B(s) := K_P + K_I/s. \quad (4)$$

Snapshots of propagating wave segments with controller (3) (see Appendix for details) are shown in Fig. 2. The reference $r(t)$ changes as a step function¹ at $t = 15$. The width $w(t)$ oscillates with a large overshoot and then converges to the reference signal $r(t) = 5$ [i.e., $e(t) \rightarrow 0$].

The PI control method has been one of the most widely used methods in the field of control engineering, since it does not require a mathematical model of the controlled object. However, in general, PI control without tuning of gains $K_{P, I}$ does not perform well, as demonstrated in Fig. 2 (see the large overshoot). If a simple mathematical model of the controlled object is derived, advanced controllers designed using the mathematical model perform well. Unfortunately, it is difficult to derive the simple model for the medium Σ . It must be emphasized that even if such a model for a specific medium can be obtained analytically, it will likely not be valid for other types of media and will have a low accuracy in practical situations.

¹The step function is generally used as the reference signal in the field of control theory [24]. Throughout this paper, we use the step function as the reference signal. We remark that our control system works well for other types of reference signals.


 FIG. 2. Snapshots and time series of wave segments [$K_P = -3 \times 10^{-3}$, $K_I = -2 \times 10^{-3}$, $z(0) = 0.093$].

III. SYSTEM IDENTIFICATION

In this section, a simple mathematical model for propagating wave segments is identified by a systematic procedure using only time series of the input signal $r(t)$ and the output signal $w(t)$. This procedure consists of collecting the time series data of the PI control system (Fig. 1) and searching for a suitable transfer function by numerical optimization. This procedure allows us to solve the above-mentioned problems. This section explains the procedure through a numerical example (Fig. 2).

Let us focus on the steady state of the control system with reference signal $r(t) \equiv w_0 = 4$ and input signal $U(t) \equiv U_0 = 0.0913$, where a wave segment with width $w(t) \equiv w_0$ propagates through the medium Σ . We suppose that the local dynamics of the control system around the steady state is governed by the linear system illustrated in Fig. 3, where the error variables from the steady state are given by

$$\begin{aligned} \Delta r(t) &:= r(t) - w_0, \quad \Delta U(t) := U(t) - U_0, \\ \Delta w(t) &:= w(t) - w_0. \end{aligned} \quad (5)$$

The medium Σ at the steady state can be described by the transfer function from the input error $\Delta U(t)$ to the output error $\Delta w(t)$

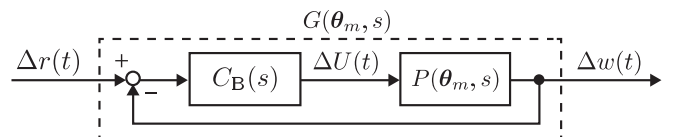


FIG. 3. Block diagram of a linear system around the steady state of the PI control system.

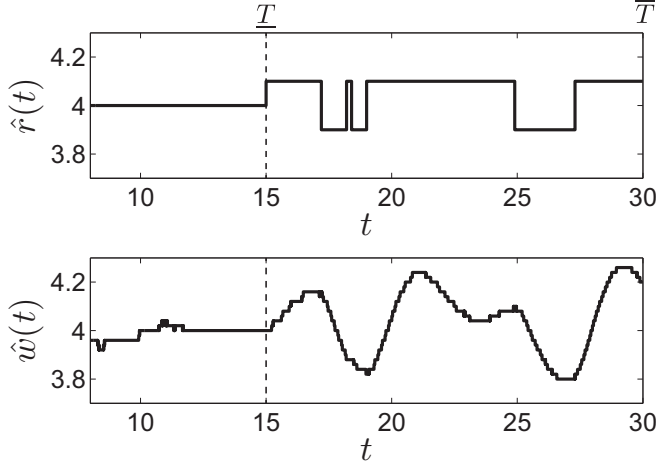


FIG. 4. Time series of the reference signal $\hat{r}(t)$ and width $\hat{w}(t)$ around the steady state ($w_0 = 4$ and $U_0 = 0.0913$) for system identification with starting time $T = 15$, finishing time $\bar{T} = 30$, and amplitude $\Delta w_0 = 0.1$.

$\Delta w(t)$,

$$P(\theta_m, s) = \frac{b_1 s^{m-1} + b_2 s^{m-2} + \dots + b_m}{s^m + a_1 s^{m-1} + a_2 s^{m-2} + \dots + a_m}, \quad (6)$$

where $\theta_m := \{a_1, a_2, \dots, a_m, b_1, b_2, \dots, b_m\} \in \mathbb{R}^{2m}$ is an unknown parameter vector and $m \in \mathbb{N}$ is the unknown degree of the transfer function. In order to estimate θ_m and m , we use the prediction-error identification method [25,26], a popular numerical approach in control engineering.

First, we collect the time series data of the PI control system, as in Fig. 1, at the steady state with $r(t) = w(t) \equiv w_0$ and $U(t) \equiv U_0$. The reference signal for system identification is set to $\hat{r}(t) = r(t) = w_0$ for $t \in [0, T]$, then it is supposed that $w(t)$ converges to w_0 by time $t = T$ as shown in Fig. 4. After that, the reference $r(t)$ is perturbed as a random binary signal $\hat{r}(t) = r(t) = w_0 \pm \Delta w_0$ for $t \in [T, \bar{T}]$, where Δw_0 is the amplitude of the binary signal. The random reference signal disturbs the width $\hat{w}(t) = w(t)$ for $t \in [T, \bar{T}]$ as shown in Fig. 4. The time series of $\hat{r}(t)$ and $\hat{w}(t)$ for $t \in [T, \bar{T}]$ are collected for the next step.

Next, we obtain the unknown θ_m and m using the collected data. The data are transformed by

$$\Delta \hat{r}(t) := \hat{r}(t) - w_0, \quad \Delta \hat{w}(t) := \hat{w}(t) - w_0. \quad (7)$$

The transformed data $\Delta \hat{r}(t)$ are used as the reference signal $\Delta r(t)$ of the linear system shown in Fig. 3: the output signal $\Delta w(t)$ is used as $\Delta w(\theta_m, t)$, which depends on the unknown θ_m and m . We try to estimate θ_m and m , which minimize the cost function:

$$J(\theta_m) = \frac{1}{\bar{T} - T} \int_T^{\bar{T}} \{\Delta \hat{w}(t) - \Delta w(\theta_m, t)\}^2 dt. \quad (8)$$

This function defines the difference between the predicted output signal $\Delta w(\theta_m, t)$ and the observed output signal $\Delta \hat{w}(t)$. We numerically try to find θ_m such that the cost function $J(\theta_m)$ is minimized:

$$\tilde{\theta}_m := \arg \min_{\theta_m} J(\theta_m). \quad (9)$$

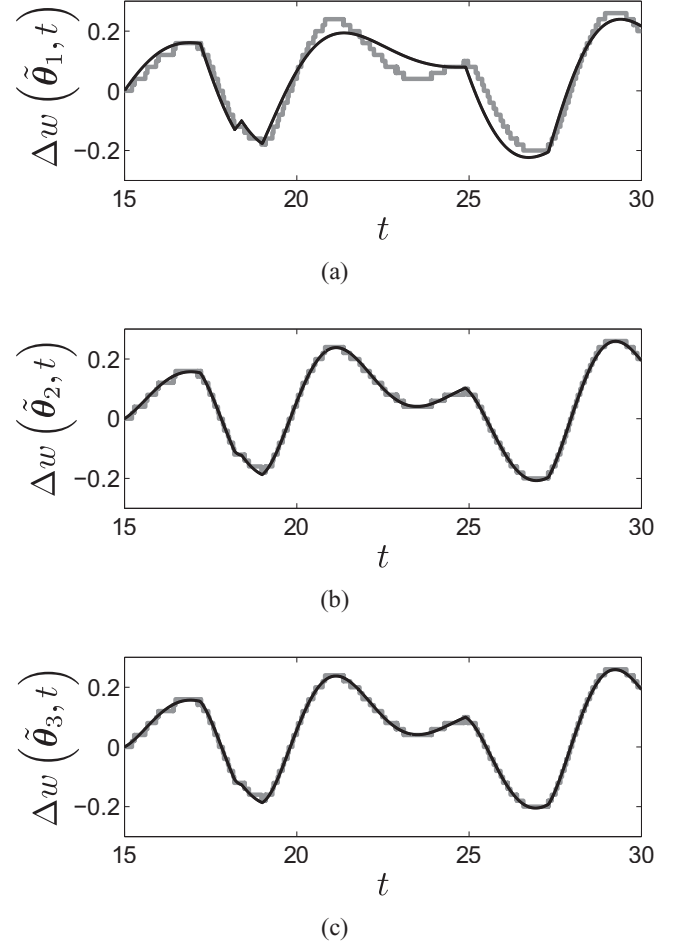


FIG. 5. Time series of the predicted output signal $\Delta w(\tilde{\theta}_m, t)$ (black line) and the observed output signal $\Delta \hat{w}(t)$ (gray line) for (a) $m = 1$, (b) $m = 2$, and (c) $m = 3$.

We use the MATLAB function *fminsearch* to find θ_m in numerical simulations. For $m = 1, 2$, and 3 , we find $\tilde{\theta}_m$ ($m = 1, 2, 3$) and obtain the transfer functions:

$$\begin{aligned} m = 1: P(\tilde{\theta}_1, s) &= \frac{-551.1}{s - 0.7417}, \\ m = 2: P(\tilde{\theta}_2, s) &= \frac{-241.9s - 721.0}{s^2 + 0.7244s - 0.1902}, \\ m = 3: P(\tilde{\theta}_3, s) &= \frac{-194.7s^2 - 1243s - 1091}{s^3 + 2.671s^2 + 0.7736s - 0.1475}, \end{aligned} \quad (10)$$

and the cost J , which minimizes the errors: $J(\tilde{\theta}_1) = 1.3947 \times 10^{-3}$, $J(\tilde{\theta}_2) = 6.4584 \times 10^{-5}$, and $J(\tilde{\theta}_3) = 6.2133 \times 10^{-5}$. The estimated parameter vector $\tilde{\theta}_m$ and the transfer functions $P(\tilde{\theta}_m, s)$ depend on the degree m . In order to determine m , we consider the cost $J(\tilde{\theta}_m)$ and the difference between the predicted output signal $\Delta w(\tilde{\theta}_m, t)$ and the observed output signal $\Delta \hat{w}(t)$ for $m = 1, 2, 3$ as shown in Fig. 5. It can be seen that for $m = 1$, the cost is high and the error is too large, but for $m = 2$ and 3 , we have a low cost and small error. As a consequence, we employ the smaller degree $m = 2$ so as to simplify the design of the control system explained below.

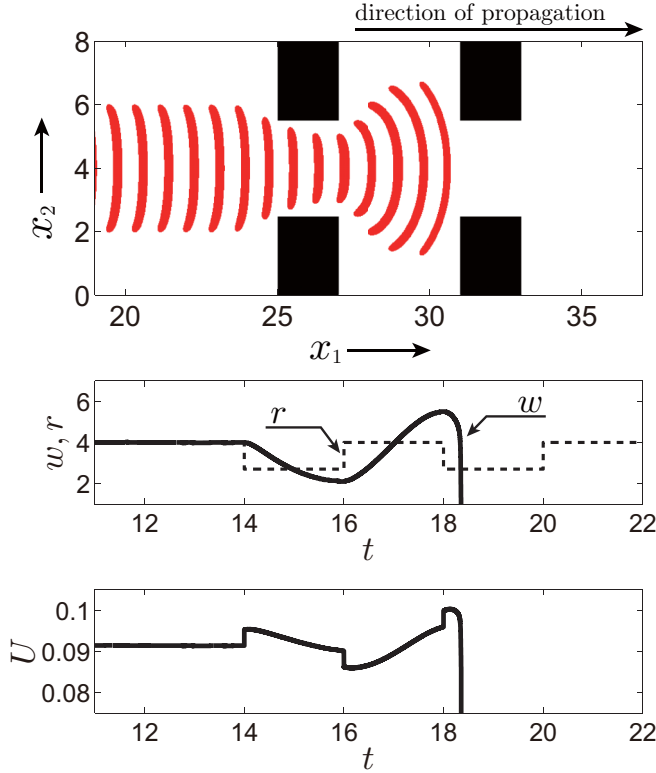


FIG. 6. Snapshots and time series of wave segments in the medium where there are two narrow channels. The parameters, initial conditions, and gains are the same as in Fig. 2.

IV. APPLICATION TO ADVANCED CONTROL

This section uses a numerical example to show how PI control confronts a problem. To solve this problem, we introduce the two-degrees-of-freedom compensation scheme [27], and we demonstrate that our control system works well in numerical simulations.

Let us consider the situation illustrated in Fig. 6, where there are four black obstacles and we want to pass the propagating wave segment through the narrow channels. The parameters and the initial conditions of the medium Σ and the gains are the same as in Fig. 2. The reference signal is varied so that it can path through the narrow channels. As seen in Fig. 6, the segment passes through the left channel but fails to pass through the right channel because the segment collapses. This collapse is induced by the rapid change and the large overshoot of the input signal U rather than a collision with the obstacles. If this rapid change and the large overshoot can be avoided, the propagating wave segment can pass through these narrow channels.

To solve this problem, we introduce the two-degrees-of-freedom compensation scheme [27]. Figure 7 is the block diagram of the control system for this scheme, where $C_B(s)$ is the feedback PI controller (4) and $C_F(s)$ is the feed-forward compensation. The linearized control system at steady state ($r(t) = w_0$ and $U(t) = U_0$) can be described by the transfer function from the reference error $\Delta r(t)$ to the output error

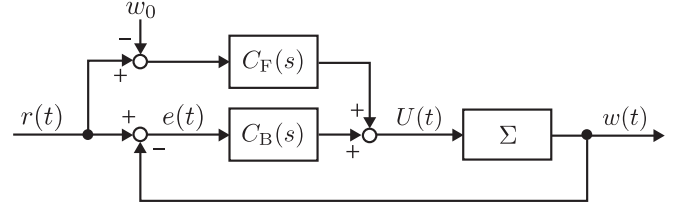


FIG. 7. Control system with feed-forward compensation.

$\Delta w(t)$:

$$G_{\Delta w - \Delta r}(s) := \frac{P(\tilde{\theta}_m, s)}{1 + P(\tilde{\theta}_m, s)C_B(s)} \{C_F(s) + C_B(s)\}. \quad (11)$$

This function governs the response of the output signal $w(t)$ to the reference signal $r(t)$; thus, if $G_{\Delta w - \Delta r}(s)$ can be adjusted to the desired transfer function $G_M(s)$, which does not induce a large overshoot, the propagating wave segment can pass through the narrow channels. Now we see that if the feed-forward compensation $C_F(s)$ is set to

$$C_F(s) = \frac{G_M(s)}{P(\tilde{\theta}_m, s)} + C_B(s)\{G_M(s) - 1\} \\ \Leftrightarrow G_{\Delta w - \Delta r}(s) = G_M(s), \quad (12)$$

then the response of $w(t)$ to $r(t)$ is described by the desired $G_M(s)$. We remark that $G_M(s)/P(\tilde{\theta}_m, s)$ has to be stable and proper to be realized.

Now we design the feed-forward compensator $C_F(s)$ in accordance with the above scheme. First, we set the desired transfer function to

$$G_M(s) = \frac{1}{(1 + \tau s)^2}, \quad \tau > 0, \quad (13)$$

which does not result in an overshoot. If we obtain the transfer function $P(\theta_2, s)$ defined by Eq. (6), the input signal with the feed-forward compensator (12) is described by

$$\begin{aligned} U(t) &= c_F z_F(t) - K_P \Delta w(t), \\ \frac{dz_F(t)}{dt} &= A_F z_F(t) + [K_I e(t) \quad 0 \quad 0 \quad \Delta r(t)]^T, \end{aligned}$$

$$c_F = \begin{bmatrix} 1 \\ \frac{a_2 + K_P b_2 - 2K_I b_2 \tau}{b_1 \tau^2} \\ \frac{a_1 + K_P b_1 - K_I(2b_1 \tau + b_2 \tau^2)}{b_1 \tau^2} \\ \frac{1 - K_I b_1 \tau^2}{b_1 \tau^2} \end{bmatrix}^T,$$

$$A_F = \begin{bmatrix} 0 & 0 & 0 & 0 \\ 0 & 0 & 1 & 0 \\ 0 & 0 & 0 & 1 \\ 0 & -\frac{b_2}{b_1 \tau^2} & -\frac{b_1 + 2b_2 \tau}{b_1 \tau^2} & -\frac{2b_1 + b_2 \tau}{b_1 \tau} \end{bmatrix}, \quad (14)$$

where $z_F(t) \in \mathbb{R}^4$ is the variable for the controller (14).

We now demonstrate our control system with the designed feed-forward compensator in numerical simulations. For the function $G_M(s)$, we set $\tau = 0.2$, and the transfer function $P(\tilde{\theta}_2, s)$ is estimated from Eq. (10). We note that $G_M(s)/P(\tilde{\theta}_2, s)$ is stable and proper. The feedback PI controller (4) has the same gains as in Figs. 2 and 6; the initial condition

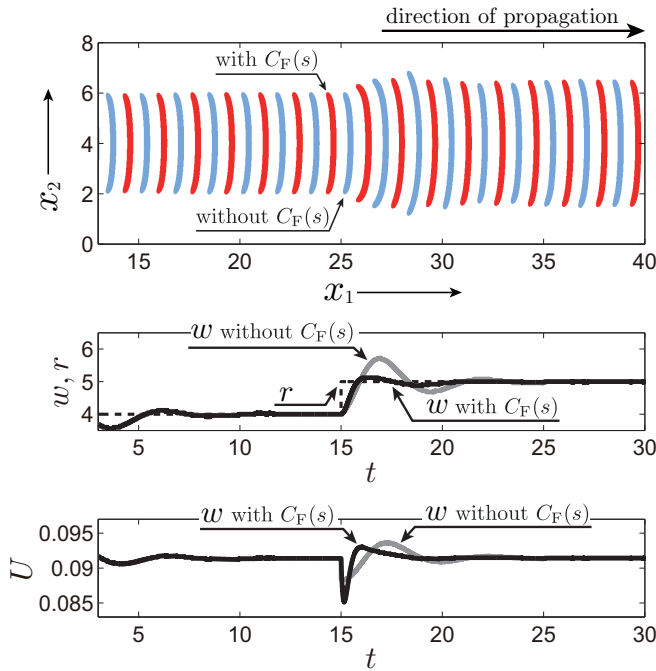


FIG. 8. Control performances of the PI control system without the feed-forward compensator $C_F(s)$ as shown in Fig. 1 and with the feed-forward compensator as shown in Fig. 7.

for controller (14) is $z_F(0) = [0.093 \ 0 \ 0 \ 0]^T$. Figure 8 shows the control performances of the PI control system with and without the feed-forward compensator $C_F(s)$. The PI control without a compensator has a large overshoot, $w(t)$; in contrast, the PI control with a compensator completely suppresses this overshoot. From this, we can see that the designed compensator works well in the numerical simulations.

Consider the PI control with compensator applied to the problem with the same parameters, initial conditions, and gains as in Fig. 6. Figure 9 demonstrates that the segment successfully passes through both the left and right channels. The width $w(t)$ responds to the reference $r(t)$ without any overshoot.

V. CONCLUSIONS

The present paper has provided an efficient scheme for controlling wave segments in excitable media. This scheme consists of two phases: the system identification phase and the advanced control phase. In the system identification phase, it is shown that, for the Oregonator model, the dynamics of propagating wave segments can be approximated by the two-dimensional transfer function. The advanced control phase effectively employs two-degrees-of-freedom compensation. Although this paper has considered only numerical simulations for the Oregonator model, the proposed scheme can potentially be applied to other types of models: similar results have been observed with the the Bär model [29] (not shown here).²

²The Oregonator model has the spatially uniform input signal U only in the function F [see Eq. (A1)]; on the other hand, the Bär model we dealt with has U only in the function $G(u, v, U) := g(u) - v + U$.

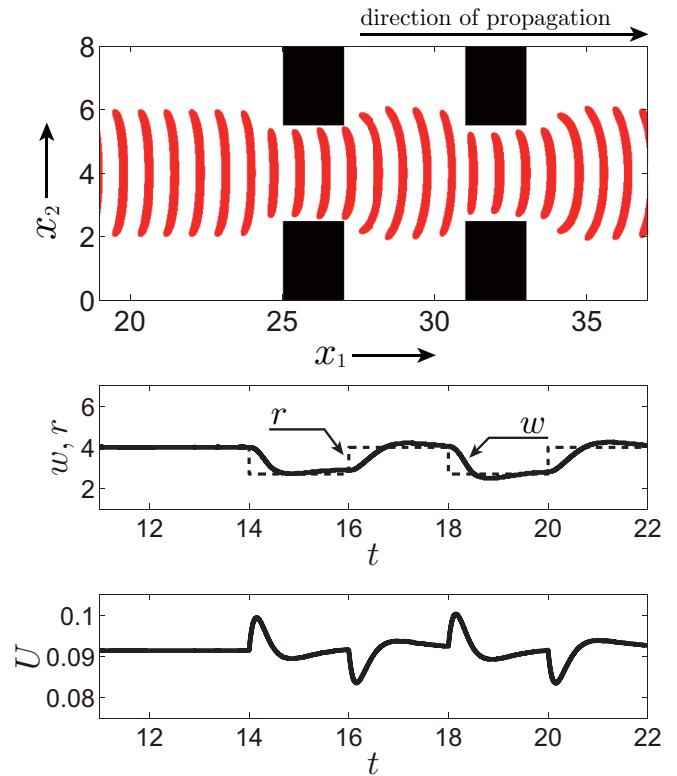


FIG. 9. Snapshots and time series of wave segments with compensator (12) in the medium with two narrow channels. The parameters, initial conditions, and gains are the same as in Fig. 6.

The system identification phase can be used in future developments for controlling reaction-diffusion systems. The numerical identification scheme is relevant for modeling a variety of reaction-diffusion systems. The simple model presented here can be used to design advanced controllers. In other words, this scheme has a potential to combine reaction-diffusion systems and a variety of advanced controllers which have been proposed already in control engineering. The present paper represents an attempt at such a combination. This combination might suggest the possibility that we can control other types of spatio-temporal nonlinear phenomena in reaction-diffusion systems by choosing suitable input and output data of phenomena.

ACKNOWLEDGMENTS

The authors would like to thank I. Yamamoto for his help in numerical simulations. The present study was partially supported by JSPS KAKENHI Grant No. JP26289131.

APPENDIX: OREGONATOR MODEL AND NUMERICAL SIMULATIONS

The Oregonator model has reaction term [17,28,30–32]

$$F(u, v, U) := \frac{1}{\epsilon} \left[u - u^2 - (av + U) \frac{u - b}{u + b} \right], \quad (A1)$$

$$G(u, v, U) := u - v,$$

where the parameters are fixed at $a = 2.5$ and $b = 0.002$. Note that the parameters fixed at $\epsilon = 0.01$ and $D = 0.1$ do not depend on position \mathbf{x} . The size of the medium is set to $L_1 = 60$ and $L_2 = 8$ throughout this paper. As an exception, we use $L_1 = 40$ in Figs. 6 and 9. The medium this paper deals

with has a no-flux boundary. We used the explicit Euler method with grid size $\Delta x = 0.02$ and time step $\Delta t = 2 \times 10^{-4}$. The threshold is set to $\bar{u} = 0.1$. The initial condition and the setup procedure are the same as Appendices A and B in our previous study [23].

-
- [1] S. Sinha and S. Sridhar, *Patterns in Excitable Media: Genesis, Dynamics, and Control* (CRC Press/Taylor & Francis, Boca Raton, FL, 2014).
- [2] D. Zipes and J. Jalife, *Cardiac Electrophysiology: From Cell to Bedside* (Saunders, Philadelphia, 2009).
- [3] I. N. Motoike, K. Yoshikawa, Y. Iguchi, and S. Nakata, *Phys. Rev. E* **63**, 036220 (2001).
- [4] A. Adamatzky, *PLoS ONE* **11**, e0168267 (2016).
- [5] A. Adamatzky, *Advances in Unconventional Computing: Prototypes, Models and Algorithms* (Springer, Cham, Switzerland, 2017).
- [6] O. Steinbock, A. Toth, and K. Showalter, *Science* **267**, 868 (1995).
- [7] S. Alonso, F. Sagues, and A.S. Mikhailov, *Chaos* **16**, 023124 (2006).
- [8] S. Alonso, F. Sagues, and A.S. Mikhailov, *Science* **299**, 1722 (2003).
- [9] H. Sakaguchi and Y. Kido, *Prog. Theor. Phys.* **161**, 332 (2006).
- [10] S. Takagi, A. Pumir, D. Pazó, I. Efimov, V. Nikolski, and V. Krinsky, *Phys. Rev. Lett.* **93**, 058101 (2004).
- [11] G. V. Osipov and J. J. Collins, *Phys. Rev. E* **60**, 54 (1999).
- [12] H. Sakaguchi and Y. Nakamura, *J. Phys. Soc. Jpn.* **79**, 074802 (2010).
- [13] M. Takeuchi, K. Konishi, and N. Hara, *Cybern. Phys.* **1**, 73 (2012).
- [14] K. Konishi, M. Takeuchi, and T. Shimizu, *Chaos* **21**, 023101 (2011).
- [15] K. Showalter and I. R. Epstein, *Chaos* **25**, 097613 (2015).
- [16] A. Mikhailov and K. Showalter, *Phys. Rep.* **425**, 79 (2006).
- [17] E. Mihaliuk, T. Sakurai, F. Chirila, and K. Showalter, *Phys. Rev. E* **65**, 065602 (2002).
- [18] A. Kothe, V. S. Zykov, and H. Engel, *Phys. Rev. Lett.* **103**, 154102 (2009).
- [19] V. S. Zykov and K. Showalter, *Phys. Rev. Lett.* **94**, 068302 (2005).
- [20] T. Sakurai, E. Mihaliuk, F. Chirila, and K. Showalter, *Science* **296**, 2009 (2002).
- [21] R. M. Tinsley, J. A. Steele, and K. Showalter, *Eur. Phys. J. Special Topics* **165**, 161 (2008).
- [22] A. J. Steele, M. Tinsley, and K. Showalter, *Chaos* **18**, 026108 (2008).
- [23] H. Katsumata, K. Konishi, and N. Hara, *Phys. Rev. E* **95**, 042216 (2017).
- [24] N. Nise, *Control Systems Engineering* (Benjamin/Cummings, Redwood, CA, 1995).
- [25] L. Ljung, *System Identification: Theory for the User* (Prentice Hall PTR, Upper Saddle River, NJ, 1999).
- [26] E. Ikonen and K. Najim, *Advanced Process Identification and Control* (Marcel Dekker, New York, NY, 2001).
- [27] B. Kuo and F. Golnaraghi, *Automatic Control Systems* (John Wiley & Sons, New York, NY, 2003).
- [28] H. J. Krug, L. Pohlmann, and L. Kuhnert, *J. Phys. Chem.* **94**, 4862 (1990).
- [29] M. Bär and M. Eiswirth, *Phys. Rev. E* **48**, R1635 (1993).
- [30] S. Kadar, T. Amemiya, and K. Showalter, *J. Phys. Chem. A* **101**, 8200 (1997).
- [31] T. Sakurai and K. Osaki, *Commun. Nonlinear Sci. Numer. Simul.* **13**, 1067 (2008).
- [32] E. Mihaliuk, T. Sakurai, F. Chirila, and K. Showalter, *Faraday Discuss.* **120**, 383 (2001).